Fatigue Behavior and Fracture Mechanism of Al Alloy 7075-T6 under Ultrasonic Cycling Deformation

Q. Chen[1, a], N. Kawagoishi[2, b], G. Hashiguchi[3, c], M. Oki[2] and K. Kusukawa[4, d]

[1]Kochi National College of Technology, 200-1 Monobe, Nankoku, 783-8508, Japan

[2]Faculty of Engineering, Kagoshima University, 1-21-40 Korimoto, Kagoshima, 890-0065, Japan

[3]Research Institute of Electronics, Shizuoka University, Hamamatsu, Shizuoka 432-8011, Japan

[4]Kochi University of Technology, Tosayamada-cho, Kochi, 782-8502, Japan

[a]qchen@me.kochi-ct.ac.jp

Keywords: Fatigue, Ultrasonic, Age-Hardened Al-Alloy, Crack Growth, Fracture Mechanism, Environmental Effect, Texture.

Abstract. To investigate the effects of loading frequency on fatigue crack growth behavior, ultrasonic fatigue tests were carried out for an extruded age-hardened Al alloy 7075-T6 in ambient air and in N_2 gas. The results obtained were compared with those in rotating bending fatigue. Fatigue strength was higher in ultrasonic fatigue than in rotating bending fatigue. This may be caused by the retardation of crack initiation and early crack propagation. In ultrasonic fatigue, the growth direction of cracks changed macroscopically from tensile mode to shear mode with the direction oblique about 35 degrees to the stress axis. Fracture mechanism involved changed from striations featured to transgranular facets and microvoids predominated. Crack growth rate at growth mode transition was ~3×10^{-9} m/cycle. The relation between applied stress, σ_a, and crack depth, b_T, at the transition sites can be approximated as $\sigma_a^n b_T$ = constant. The results were discussed from viewpoints of crack tip plasticity, time dependent environment effect and the texture microstructure of the alloy.

Introduction

In the last decades, fatigue properties of metallic materials in very high cycle life regime have attracted intensive attentions for the purpose of securing the reliability of machines served for a lifespan of 10-20 years or estimating the residual life of ageing structures beyond design life. Many researches focused on high strength steels and surface hardened steels and some interesting results have been found. For example, internal fracture took place at lower stress levels than the conventional fatigue limit and beyond life region of 10^7 cycles, leading to the featured step-wise endurance curves [(1),(2)]. The mechanisms involved in internal fracture, however, have not been elucidated yet. On the other hand, fatigue tests in gigacycle regime are time-consuming and expensive to conduct, and accelerated fatigue testing methods were demanded.

Ultrasonic fatigue was introduced as an accelerated fatigue tool in 1950, and has found increasing applications in exploring ultra long life for various kinds of metals [(3),(4)], though the validity of ultrasonic methodology or the effects of ultrasonic frequency on fatigue properties were concerned. It was reported that in the case of a bearing steel SNCM439 [(5)] and a Ti based alloy [(6)], fatigue strength increased under ultrasonic loading if fracture was surface cracking dominated, but it was hardly affected when internal cracking from defects happened. In our recent studies on nickel based superalloy Inconel 718 [(7)], however, fatigue strength of plain specimen increased while subjecting to ultrasonic cyclic deforming. Meanwhile, the influence of environment on fatigue strength can hardly be neglected, especially for high strength alloys [(8), (9)].

The objective of the present study, therefore, is to investigate the effects of ultrasonic frequency on the crack growth behavior of age-hardened Al alloy 7075-T6 in ambient air and in N_2 gas. The

fracture mechanism involved will be examined through subsequent surface observation as well as scanning electron microscopic analysis.

Materials and Experimental

The material used was an extruded bar of age-hardened Al alloy 7075-T6. The chemical composition (wt. %) of the alloy is 0.09Si, 1.47Cu, 0.25Fe, 0.03Mn, 2.56Mg, 0.19Cr, 5.46Zn, 0.03Zr, 0.03Ti, and the remainder Al. The mechanical properties of the alloy are 630 MPa of 0.2% proof stress, 691 MPa of tensile strength, 764 MPa of true fracture strength, and 9.5% of area reduction, respectively.

All of the specimens were electrochemically polished by ~20 μm in surface depth after emery paper grinding in order to reduce the effect of worked layer and for better surface damage observation. The observation of fatigue damage development and the measurement of surface crack length were conducted directly under a scanning electron microscope (SEM) or under an optical microscope by using plastic replica technique. Crack length, l, was measured on the surface of the specimens in circumferential direction. In the case of specimens with a blind hole, the diameter of the hole was included in the measured crack length.

The machines employed were a 19.5 KHz piezoelectricity actuated ultrasonic fatigue system developed in our group, and an Ono-type rotating bending fatigue machine with a capacity of 100Nm, operating at 50Hz. Fatigue experiments were carried out at room temperature and stress ratio of $R = -1$, in laboratory atmosphere or in nitrogen gas environment. To minimize internal friction induced temperature rise, ultrasonic fatigue tests were performed in a pulse-pause manner with a pulse length of 1 s and pause time of 5 s. The maximum temperature rise was less than 3°C during the ultrasonic fatigue process. The details of the ultrasonic fatigue and rotating bending fatigue tests can be found in the literatures [7]. Fatigue experiments in the nitrogen gas environment were conducted within a vinyl chamber in which nitrogen gas of at least 99.995% purity was supplied with the contents of oxygen and water vapor controlled below 5 ppm and 10 ppm, respectively.

Results and Discussion

Fig. 1 shows the *S-N* curves of plain and drilled specimens subjected to ultrasonic (U) and rotating bending (R.B) cycles with the data of plain specimens quoted from our previous study [9]. In case of plain specimens, fatigue life is longer under ultrasonic fatigue than under rotating bending fatigue, this is especially true when taking into account the considerable sectional stress gradient occurred during rotating bending cycles. Similar tendency is seen in the drilled specimens too, though the effect of ultrasonic loading on the fatigue life is less remarkable, comparing to that in the plain specimens.

Fig. 2 presents absolutely different crack propagation paths observed in the drilled specimens, characteristic of crack growth behavior in the alloy during (a) ultrasonic fatigue and (b) rotating bending fatigue. As reported previously [9], crack growth under rotating bending fatigue was mostly tension stress dominated whereas under ultrasonic fatigue, crack growth transited from tension mode to shear mode beyond extending some distance. The angle between the shear mode cracks and the stress axle is ~35 degrees. These observations did not change with the existence of the blind hole as well as the level of loading stresses.

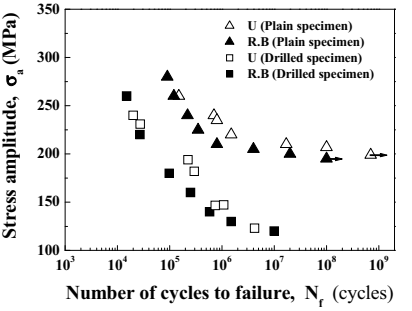

Fig. 1 Endurance curves in air

Fig. 3 shows fracture morphologies observed in a drilled specimen failed under ultrasonic fatigue. Differing from major striations that feature tension mode crack propagation in the traditional rotating bending fatigue, striations can be merely found in the region corresponding to tension mode controlled crack growth. However, in the shear mode extension area, slip bands along with characteristic voids that distributed on these slip bands are of particular interests, since they were never observed in any specimens that failed during rotating bending fatigue.

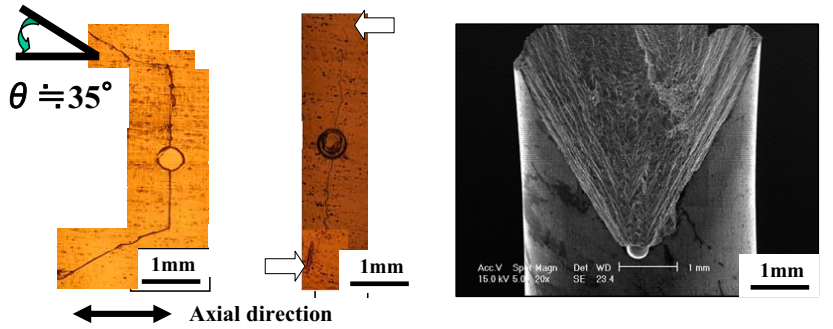

(a) Ultrasonic fatigue
σ_a = 146MPa
N_f = 7.4×10^5 cycles

(b) Rotating bending
σ_a = 220 MPa
N_f = 2.5×10^4 cycles

(c) SEM micrograph under ultrasonic fatigue
σ_a = 194 MPa, N_f =.2.2×10^5 cycles

Fig. 2 Crack morphology under ultrasonic fatigue in air

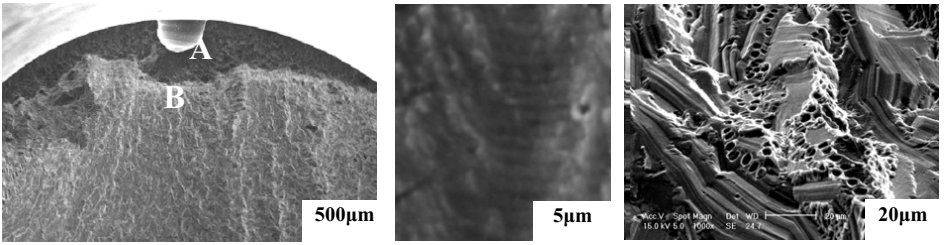

(a) Whole view (b) Part A in (a) (c) Part B in (a)

Fig. 3 Fracture surface under ultrasonic fatigue in air (σ_a = 124 MPa, N_f = 4.20×10^6 cycles)

The effect of ultrasonic frequency on crack growth behavior was investigated by using plain specimens. Fig. 4 shows the relation of crack length as a function of loading cycles. The transition of crack growth mode was confirmed not only on the surface crack traces but also on the fracture morphology, as shown in Fig. 3(c). In the present study, crack length, l, was defined as projection length to the circumferential direction on the surface, thus the arrows in Fig. 4 indicate the occurrence of crack growth mode transition on the surface. Significant delay is recognized in the crack initiation or the early crack growth under ultrasonic fatigue. Actually, crack initiation took place during 20 - 40% of fatigue life and the majority of fatigue life was consumed to advance cracks, irrespective of loading frequency. Therefore, the main reason for the life elongation under ultrasonic fatigue is due to the suppression of crack initiation and early crack growth.

Fig. 5 shows the relationship of crack growth rate as a function of stress intensity factor range, ΔK. In case of ultrasonic fatigue, σ_a was determined by the displacement at free end of the specimen [7]. The aspect ratio of crack depth to surface crack length was ~0.4 for cracks propagating in tension mode under rotating bending fatigue. The aspect ratio in ultrasonic fatigue, however, varied a little between the plain and the drilled specimens and was uncertain due to the complex fracture morphology after crack growth transited from tension mode to shear one. For the convenience of ΔK calculation, therefore, a half of surface crack length was employed. Crack growth data obtained for long cracks under ultrasonic fatigue [10], was also included for comparison with the mean crack growth rate under rotating bending fatigue and ultrasonic fatigue represented by a dashed and a solid lines, respectively. It can be seen that a crack propagates slower in ultrasonic fatigue than in rotating bending fatigue if ΔK is less than a critical value of ~6-8 MPa$\sqrt{m}$. However, ultrasonic fatigue cracks grow faster at larger ΔK, i.e. ΔK > 6-8 MPa$\sqrt{m}$.

As arc-marked in Fig. 3a, crack morphology related to tension mode growth (part A) is totally different from that under shear mode growth (part B), so that crack depth corresponding to the transition point of crack growth from tension mode to shear mode is of particular interest in the ultrasonic fatigue of the alloy. In Fig. 6, the crack depth at the transition point is plotted with the stress amplitude applied. The lower the stress applied, the deeper the crack depth at transition point. In fact, the relation between the crack depth at transition point, b_T and the applied stress, σ_a, can be linearly approximated as $\sigma_a^n b_T = C$, where n and C are constants depending on material properties and loading conditions, implying there exists a mechanical criteria that determines the growth mode transition under ultrasonic fatigue.

Fig. 6 shows the relation between the stress intensity factor range at transition point, ΔK_T, and ultrasonic fatigue life, N_f, in which ΔK_T was determined by following the method described in reference [11]. Although ΔK_T derivates to some extents, it converges to ~8 MPa$\sqrt{m}$.

Discussion

As mentioned above, fatigue life was longer under ultrasonic fatigue than under rotating bending fatigue, which is a definite effect of loading frequency on the fatigue life of Al alloy 7075-T6. Meanwhile, surface observation suggests that the suppression of crack initiation as well as the early propagation of small cracks be related to the extension of fatigue life under ultrasonic fatigue (Fig. 4). The flow stress increase in metallic materials due to high strain rate cycling [12], is one of the possible reasons.

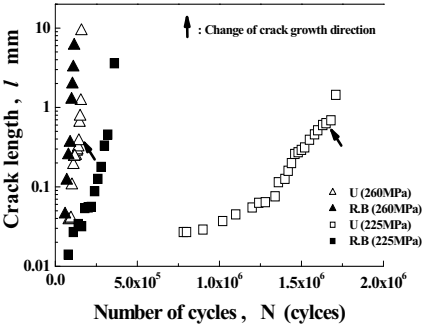

Fig. 4 Crack growth curves in air

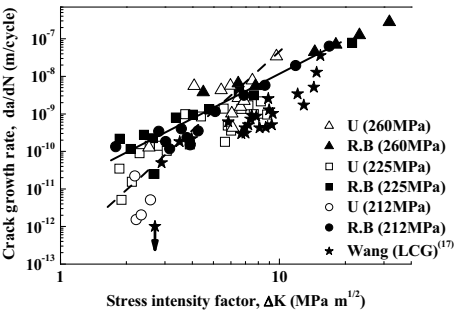

Fig. 5 Crack growth rate as a function of ΔK_T

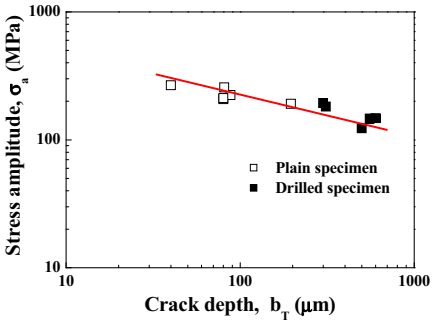

Fig. 6 σ_a as a function of b_T

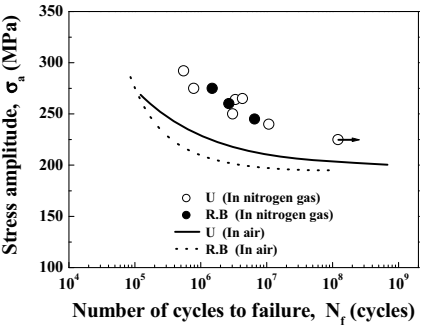

Fig. 7 Endurance curves in N_2 gas

On the other hand, the transition of crack growth mode from tension to shear may be correlated to the characteristic microstructure of crystal clusters formed during the extrusion process of the alloy, because the macroscopic crack extension under shear mode was ~35 degree to the stress axle or extrusion direction, which matches well with the angle of 35.7 degree formed between slip planes {111} and extrusion planes {110} along the axial direction [13]. This is true because numerous voids oriented from precipitates were observed on specific planes and facets (Fig. 3c), and that precipitates preferred to distribute on the planes {111} and {110} [14].

The transition of crack growth from tension mode to shear mode was well investigated for extruded Al alloys, and it was reported that the transition may take place if the crack tip plasticity region reaches 4 times as large as mean grain size [15]. Actually, the nearly constant ΔK_T (Fig. 8) imposes the existence of such a mechanical condition for the growth mode transition to happen in the conditions of present study. However, it is difficult by using only a mechanical parameter, ΔK_T, to explain why this kind of crack growth transition did not occur in the rotating bending fatigue of the alloy in air. Other effects besides ΔK_T, e.g. environmental influence, have to be taken into account.

It is well known that the diffusion of oxygen and moisture and the surface reaction kinetics ahead of crack tip are time dependent, and hence the effects of ambient air on crack propagation behavior at ultrasonic frequency are crack growth rate controlled in the light of competition between the advance of crack tip per cycle and the distance reachable by oxygen and moisture molecules during a cycle. In ultrasonic fatigue, for instance, the cyclic opening and closure behavior at crack tip in ambient air can be quite similar to that in vacuum and differed fracture mechanism may arise, provided that crack growth rate exceeds the diffusion speed of moisture molecules so as to avoid them from getting into fresh surfaces at crack tip [16]. In case of Al alloys, the cutoff crack growth rate was found to be ~3×10^{-9} m/c [17]. As seen in Fig. 5, crack growth rates associated with the critical stress intensity factor range at transition point in ultrasonic fatigue, i.e. ΔK= ~8 MPa$\sqrt{m}$, fall in the range of 2-3×10^{-9} m/c, which agrees well to the above-mentioned cutoff rate. On the other hand, similar sharp change in crack paths as seen in the ultrasonic fatigue (Fig. 3(a)), was also observed in the rotating bending fatigue of extruded Al alloys in a condition lacking of oxygen and moisture [18] and in oil environment [19]. It is clear that environment at crack tip, especially the absorption of oxygen and moisture during each loading cycle, become a key factor to determine the crack growth transition of Al alloys in lab atmosphere.

Fig. 7 shows *S-N* curves of plain specimens fatigued in nitrogen environment. In Fig. 7, the results obtained in ambient air are represented as line graphs for comparison. The prominent life dependence on loading frequency as observed in ambient air environment diminishes in the fatigue in nitrogen. Furthermore, fatigue strength increases significantly in nitrogen than in air, irrespective of loading

frequency. Some fatigue experiments in nitrogen gas was interrupted after stress cycling beyond the fatigue life of plain specimens failed in air. Crack initiation, however, was not recognized on the surface of either ultrasonic or rotating bending fatigued specimens. Considering the facts that crack nucleation seldom happened before ~40% of total life in the fatigue of the alloys in air, a delay in fatigue crack nucleation may be the main reason that gives rise to the large life increase in both ultrasonic and rotating bending fatigue in nitrogen gas.

Usually, variation of surface energy due to moisture and oxygen absorption is considered to affect crack initiation. In the present study, the exactly same surface treatment was carried out for the specimens prior to fatigue in nitrogen gas as in air, so that the influence of initial surface conditions, e.g. moisture and oxygen absorption, on fatigue slip deformation as well as crack nucleation would not differ meaningfully in nitrogen environment from that in ambient air. Further research, however, is necessary to elucidate surface energy variation during stress cycling in nitrogen gas and the main causes that led to crack initiation suppression in both ultrasonic and rotating bending fatigue in nitrogen gas.

Crack morphology and fracture surface were analyzed for the specimens fatigued in nitrogen gas. In case of ultrasonic fatigue, crack growth transited from tension mode to shear one in nitrogen gas (Fig. 8a), similar to that observed in ambient air (Fig. 4). However, crack advance under tension mode is much shorter, and the striations characteristic of tensile crack propagation are less recognized in nitrogen gas than in ambient air, as shown in Fig. 9b.

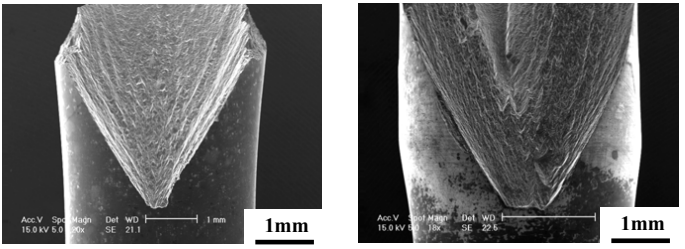

(a) Ultrasonic fatigue (σ_a = 265MPa, N_f = 4.30×10^6 cycles)

(b) Rotating bending fatigue (σ_a = 245MPa, N_f = 6.57×10^6 cycles)

Fig. 8 Crack morphology in N_2 gas

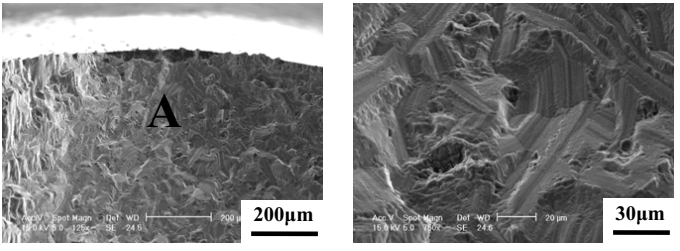

(a) Whole view

(b) Part A in (a)

Fig. 9 Fracture micrograph of specimen subjected to ultrasonic fatigue in N_2 gas (σ_a = 265MPa, N_f = 4.30×10^6 cycles)

In case of rotating bending fatigue, however, shear mode crack growth that was not observed in ambient air, was recognized obviously in nitrogen gas with almost the same inclination of ~35 degrees to the stress axle as seen in ultrasonic fatigue (Fig. 8b). Furthermore, no significant frequency influence on the fracture mechanism of the Al alloy was recognized in nitrogen gas, as seen in Figs. 9 and 10.

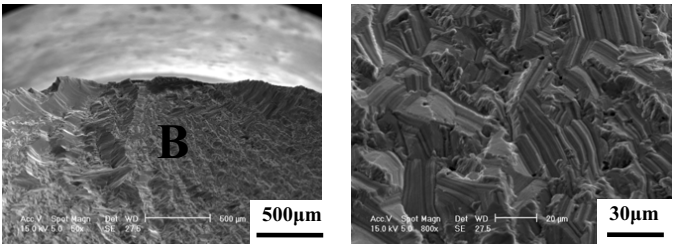

(a) Whole view (b) Part B in (a)

Fig. 10 Fracture micrograph of specimen subjected to rotating bending fatigue in N_2 gas ($\sigma_a = 245$MPa, $N_f = 6.57 \times 10^6$ cycles)

As mentioned above, the fatigue strength of the plain specimens in ambient air is higher in ultrasonic fatigue than in rotating bending fatigue (Fig. 7). The main reason for the strength increase in ultrasonic fatigue was considered to be due to flow stress rise during high strain rate deforming such that crack initiation in ultrasonic fatigue was significantly suppressed. Similar trend would have appeared in the fatigue of the alloy in nitrogen gas, in which no distinguished life difference was found between ultrasonic and rotating bending fatigue. Stress gradient in rotating bending fatigue, which lightened remarkably damage degree in the vicinity of small cracks, is concerned as a primary factor that can cancel the increased flow stress induced life advantage in ultrasonic fatigue.

Consequently, the transition in crack growth mode as well as in fracture mechanism is possible in both ultrasonic and rotating bending fatigue of the Al alloy. The transition depends not only on the mechanical relation between crack tip plasticity field and grain size, but also on the competition between crack extension per cycle and the diffusion rate of oxygen and moisture into crack tips. The latter is more important.

Conclusions

Ultrasonic and rotating bending fatigue experiments were carried out with Al alloy 7075-T6 at room temperature in ambient air and in nitrogen gas. Fatigue crack growth behavior and fracture mechanism involved were investigated and the effects of loading frequency were examined from the viewpoints of environment and microstructure. The following results are concluded.

In case of fatigue in ambient air condition, fatigue life was longer in ultrasonic fatigue than in rotating bending fatigue. Differing from the tension mode dominated failure in rotating bending fatigue, crack growth in ultrasonic fatigue transited macroscopically from tensile extension characteristic of striations to shear advance featured by facets. The direction of macroscopic shear mode crack propagation inclined ~35 degrees to the stress axle. In ultrasonic fatigue, the crack depth at the crack growth transition point increased with decrease in loading stress. The relation can be approximated as $\sigma_a^n b_T = 4$. The cutoff crack growth rate at transition point was found to be ~3×10^{-9} m/c and the associated critical stress intensity factor range was ~8 MPa$\sqrt{m}$ .Cracks grew slower in

ultrasonic fatigue than in rotating bending fatigue before the transition happened, and grew faster after then.

In case of fatigue in nitrogen gas condition, the difference in fatigue life between ultrasonic and rotating bending fatigue decreased and was less remarkable than in ambient air condition. Crack growth in ultrasonic fatigue transited similarly from tensile extension to shear advance as in ambient air. Macroscopic shear mode crack growth transition happened in rotating bending fatigue with almost the same inclination of ~35 degrees to the stress axle as seen in ultrasonic fatigue. Environment, e.g. the diffusion of moisture and oxygen at crack tip, played an important role in the macroscopic shear mode crack growth transition of the alloy. The transition direction of shear mode crack growth in the alloy has a close relation with the texture structure of the alloy.

Acknowledgments

The authors are grateful to Mrs. N. Yoneyama, T. Arima, K. Yoshinaga, and K. Hagiwara for their technical supports.

References

[1] Murakami, Y. et al., Trans. JSME, Series A, Vol.66, No.642 (2000), pp.311-319.

[2] QY. Wang, et al., International Journal of Fatigue, Vol.24(2002), pp.1269-1274.

[3] C. Bathias, Fatigue Fracture Engng Materials Structures, Vol.22 (1999), pp.559-565.

[4] S. E. Stanzl-Tschegg, H. Mayer, International Journal of Fatigue, Vol.23 (2001), pp.231-237.

[5] Furuya, Y. et al., Trans. JSME, Series A, Vol.68, No.667 (2002), pp.477-483.

[6] Takeuchi, E. et al., Trans. JSME, Series A, Vol.70, No.696 (2004), pp.1124-1130.

[7] Q. Chen, et al., (2005), International Journal of Fatigue, Vol.27, pp. 1227-1232.

[8] R.P. Wei, et al., Metallurgical Transactions A, 11A (1980), pp.151-158.

[9] N. Kawagoishi, et al., Trans. JSME, Series A, Vol.69, No.688(2003), pp.1672-1677.

[10] Wang, QY., et al., Scripta Materialia, Vol.48(2003), pp.9-14.

[11] Nisitani, H., Chen, D-H., Trans. JSME, Series A, Vol.50, No.453 (1984), pp.1077-1083.

[12] Miura, K. et al., J. the Society of Materials Science, Japan, Vol.47 (1998), pp.1053-1058.

[13] The Japan Society of Materials Science ed., Materials, Mechanical Properties and Testing Methods (in Japanese), 1981, p.55.

[14] The Japan Society of Light Metals ed., Microstructures and Properties of Aluminums (in Japanese), 1990, p.302.

[15] R. Koterazawa, D. Shimo, J. the Society of Materials Science, Japan, Vol.25 (1976), pp.535-54.

[16] J.K. Tien, R.P. Gamble, Metallurgical Transactions, Vol.2(1971), pp.1933-1938.

[17] B. Holper, et al., International Journal of Fatigue, 25(2003), pp.397-411.

[18] T. Okada, et al., J. the Society of Materials Science, Japan, Vol.31 (1982), pp.383-389.

[19] N. Kawagoishi, H. Nisitani, Trans. JSME, Series A, Vol.55, No.512 (1989), pp.703-709.